J. Fluid Mech. (2006), *vol.* 551, *pp.* 185–195. © 2006 Cambridge University Press
doi:10.1017/S0022112005007950 Printed in the United Kingdom

Maximum drag reduction asymptotes and the cross-over to the Newtonian plug

By R. BENZI[1], E. DE ANGELIS[2], V. S. L'VOV[3], I. PROCACCIA[3] AND V. TIBERKEVICH[3]

[1]Dipartimento di Fisica and INFN, Università "Tor Vergata", Via della Ricerca Scientifica 1, I-00133, Roma, Italy

[2]Dipartimento Mecc. Aeron., Università di Roma "La Sapienza", Via Eudossiana 18, 00184, Roma, Italy

[3]Department of Chemical Physics, The Weizmann Institute of Science, Rehovot, 76100 Israel

(Received 13 May 2004 and in revised form 12 September 2005)

We employ the full FENE-P model of the hydrodynamics of a dilute polymer solution to derive a theoretical approach to drag reduction in wall-bounded turbulence. We recapture the results of a recent simplified theory which derived the universal maximum drag reduction (MDR) asymptote, and complement that theory with a discussion of the cross-over from the MDR to the Newtonian plug when the drag reduction saturates. The FENE-P model gives rise to a rather complex theory due to the interaction of the velocity field with the polymeric conformation tensor, making analytic estimates quite taxing. To overcome this we develop the theory in a computer-assisted manner, checking at each point the analytic estimates by direct numerical simulations (DNS) of viscoelastic turbulence in a channel.

1. Introduction

The onset of turbulence in fluid flows is accompanied by a significant increase in the drag (Lumley 1969; Sreenivasan & White 2000). This drag is a hindrance to the transport of fluids and to the navigation of ships. It is of interest therefore that the addition of long chain polymers to wall-bounded turbulent flows can result in a significant reduction in the drag. The basic experimental knowledge of the phenomenon had been reviewed and classified by Virk (1975); the amount of drag depends on the characteristics of the polymer and its concentration, but cannot exceed a universal asymptote known as the 'maximum drag reduction' (MDR) curve which is independent of the polymer's concentration or its characteristics. When the concentration is not large enough, the mean velocity profile as a function of the distance from the wall follows the MDR curve for a while and then crosses back to a Newtonian-like profile, cf. figure 1(*a*). The coordinates used in the figure are the standard Prandtl wall units (with p' being the pressure gradient and L half the channel height, $V^+ \equiv V/\sqrt{p'L}$, $y^+ \equiv \sqrt{p'L}yL/\nu_s$, and ν_s the kinematic viscosity).

Recently the nature of the MDR and the mechanism leading to its establishment were rationalized, using a phenomenological theory in which the role of the polymer conformation tensor was modelled by an effective viscosity (L'vov *et al.* 2004). The effective viscosity was found to attain a self-consistent profile, increasing linearly with the distance from the wall. With this profile the reduction in the momentum flux from the bulk to the wall overwhelms the increased dissipation that results from the increased viscosity. Thus the mean momentum increases in the bulk, and this is how

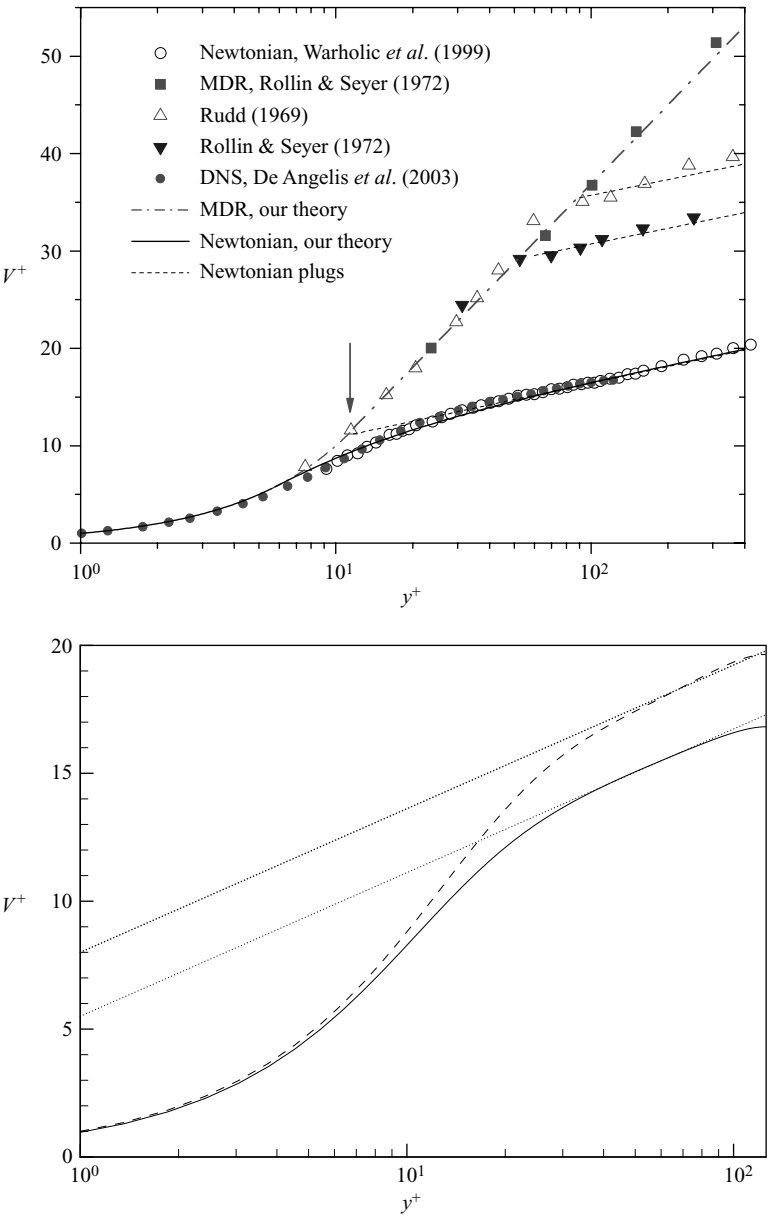

FIGURE 1. (*a*) Mean normalized velocity profiles as a function of the normalized distance from the wall during drag reduction. The data points from numerical simulations (filled circles) and the experimental points (open circles) represent the Newtonian results. The squares represent the maximum drag reduction (MDR) asymptote. The dashed curve represents the theory discussed in the paper which agrees with the universal MDR. The arrow marks the crossover from the viscous layer to the Newtonian log-law of the wall. The filled triangles and open triangles represent the cross-over, for intermediate concentrations of the polymer, from the MDR asymptote to the Newtonian plug. (*b*) Mean velocity profiles for the Newtonian and for the viscoelastic simulations with $Re_\tau = 125$, where Re_τ is the Reynolds number based on the friction velocity. Solid line: Newtonian, dashed line: viscoelastic. The straight lines represent the classical von-Kármán log-law. Notice that in this simulation the modest Reynolds number results in an elastic layer in the region $y^+ \leqslant 25$.

drag reduction is realized. In De Angelis *et al.* (2004) it was shown by direct numerical simulations (DNS) that Navier–Stokes flows with viscosity profiles that vary linearly with the distance from the wall do indeed show drag reduction in close correspondence with the phenomenon seen in full viscoelastic simulations. The aim of this paper is to complement the simplified theory with a derivation of the same results on the basis of a full viscoelastic model of the hydrodynamics of dilute polymer solutions. Such a derivation loses some of the simplicity of the phenomenological theory, but on the other hand it clarifies the role of the polymer conformation tensor in providing viscosity-like contributions. In addition, we will offer a discussion of the non-universal saturation of drag reduction as a function of concentration, length of polymer and relaxation time in various conditions of experimental interest. In § 2 we consider the FENE-P model of viscoelastic flows and briefly review the evidence for drag reduction in DNS of this model. In § 3 we employ the FENE-P model to derive a statistical theory of drag reduction in wall-bounded turbulence. In § 4 we use the theory to predict the cross-over from the universal MDR to the Newtonian plug when the conditions differ from those necessary for attaining the MDR. In § 5 we present a summary and a discussion.

2. Equations of motion for viscoelastic flows and drag reduction

Viscoelastic flows are represented well by hydrodynamic equations in which the effect of the polymer enters in the form of a 'conformation tensor' $R_{ij}(r,t)$ which stems from the ensemble average of the dyadic product of the end-to-end distance of the polymer chains (Bird *et al.* 1987; Beris & Edwards 1994). A successful model that had been employed frequently in numerical simulations of turbulent channel flows is the FENE-P model (Bird *et al.* 1987). Flexibility and finite extensibility of the polymer chains are reflected by the relaxation time τ and the Peterlin function $P(r,t)$ which appear in the equation of motion for R_{ij}:

$$\frac{\partial R_{\alpha\beta}}{\partial t} + (U_\gamma \nabla_\gamma) R_{\alpha\beta} = \frac{\partial U_\alpha}{\partial r_\gamma} R_{\gamma\beta} + R_{\alpha\gamma} \frac{\partial U_\beta}{\partial r_\gamma} - \frac{1}{\tau}[P(r,t) R_{\alpha\beta} - \delta_{\alpha\beta}], \tag{2.1}$$

$$P(r,t) = \left(\rho_m^2 - 1\right) \Big/ \left(\rho_m^2 - R_{\gamma\gamma}\right). \tag{2.2}$$

Here and below repeated indices are summed. In these equations ρ_m^2 refers to the maximal of the trace $R_{\gamma\gamma}$ in units of ρ_m^2. Since in most applications $\rho_m \gg 1$ the Peterlin function can also be written approximately as

$$P(r,t) \approx (1/(1 - \alpha R_{\gamma\gamma}), \tag{2.3}$$

where $\alpha = \rho_m^{-2}$. In turn the conformation tensor appears in the equations for fluid velocity $U_\alpha(r,t)$ as an additional stress tensor:

$$\frac{\partial U_\alpha}{\partial t} + (U_\gamma \nabla_\gamma) U_\alpha = -\nabla_\alpha p + \nu_s \nabla^2 U_\alpha + \nabla_\gamma T_{\alpha\gamma} + F_\alpha, \tag{2.4}$$

$$T_{\alpha\beta}(r,t) = \frac{\nu_p}{\tau}[P(r,t) R_{\alpha\beta}(r,t) - \delta_{\alpha\beta}]. \tag{2.5}$$

Here ν_s is the viscosity of the pure fluid, F_α is the forcing and ν_p is a viscosity parameter which is related to the concentration of the polymer, i.e. $\nu_p/\nu_s \sim c_p$ where c_p is the volume fraction of the polymer. We note however that the tensor field can be rescaled to get rid of the parameter α in the Peterlin function, $\tilde{R}_{\alpha\beta} = \alpha R_{\alpha\beta}$, with the only consequence being rescaling the parameter ν_p accordingly. Thus the value of the concentration can be calibrated against the experimental data. Also, in most

numerical simulations, the term $PR_{\alpha\beta}$ is much larger than unity. Therefore, in the theoretical development below we shall use the approximation

$$T_{\alpha\beta} \sim \frac{\nu_p}{\tau} PR_{\alpha\beta}. \tag{2.6}$$

These equations were simulated by computer in a channel or pipe geometry, reproducing the phenomenon of drag reduction in experiments. The most basic characteristic of the phenomenon is the increase of fluid throughput in the channel for the same pressure head, compared to the Newtonian flow. This phenomenon is demonstrated in figure 1(*b*) taken from De Angelis *et al.* (2003). As one can see the simulation is limited compared to experiments; the Reynolds number is relatively low, and the MDR is not attained. Nevertheless the phenomenon is shown, and we will be able to use the simulation to asses and support the steps taken in the theoretical development.

3. The derivation of the MDR

3.1. *The momentum balance equation and closure approximations*

Consider the fluid velocity $U_\alpha(r)$ as a sum of its (time) average and a fluctuating part:

$$U_\alpha(r,t) = V_\alpha(y) + u_\alpha(r,t), \qquad V_\alpha(y) \equiv \langle U_\alpha(r,t)\rangle. \tag{3.1}$$

For a channel of large length and width all the averages, and in particular $V_\alpha(y) \to V(y)\delta_{\alpha y}$, are functions of y only. The parameters that enter the theory are the mean shear $S(y)$, the Reynolds stress $W(y)$, the kinetic energy $K(y)$ and the mean conformation tensor $\langle R_{\alpha\beta}\rangle$; the first three are defined respectively as

$$S(y) \equiv \mathrm{d}V(y)/\mathrm{d}y, \quad W(y) \equiv -\langle u_x u_y\rangle, \quad K(y) = \langle u_\alpha u_\alpha\rangle/2.$$

Taking the long-time average of (2.4), and integrating the resulting equation along the y coordinate produces an exact equation for the momentum balance:

$$W + \nu S + \frac{\nu_p}{\tau}\langle PR_{xy}\rangle(y) = p'(L-y). \tag{3.2}$$

The right-hand side is simply the rate at which momentum is produced by the pressure head, and on the left-hand side we have the Reynolds stress which is the momentum flux, the viscous dissipation of momentum and the rate at which momentum is transferred to the polymers. Near the wall it is permissible to neglect the term $p'y$ on the right-hand side for $y \ll L$. In order to proceed, we need to use (2.1) in its averaged form:

$$\frac{\partial}{\partial y}\langle u_y R_{ij}\rangle = -\frac{1}{\tau}\langle PR_{ij}\rangle + \langle R_{ik}\partial_k U_j\rangle + \langle R_{jk}\partial_k U_i\rangle. \tag{3.3}$$

Using $\langle \partial_k U_j\rangle \equiv S\delta_{jx}\delta_{ky}$, we can rewrite equation (3.3) in the form

$$\frac{1}{\tau}\langle PR_{ij}\rangle = \langle R_{ik}\rangle S\delta_{jx}\delta_{ky} + \Phi_{ij} \tag{3.4}$$

where $\Phi_{ij} \equiv -\partial_y\langle u_y R_{ij}\rangle + \langle R_{ik}\partial_k u_j\rangle + \langle R_{jk}\partial_k u_i\rangle$. In particular we obtain the following equations for R_{xx}, R_{xy}:

$$\langle PR_{xx}\rangle = \tau S\langle R_{xy}\rangle + \tau\Phi_{xx}, \tag{3.5}$$

$$\langle PR_{xy}\rangle = \tau S\langle R_{yy}\rangle + \tau\Phi_{xy}. \tag{3.6}$$

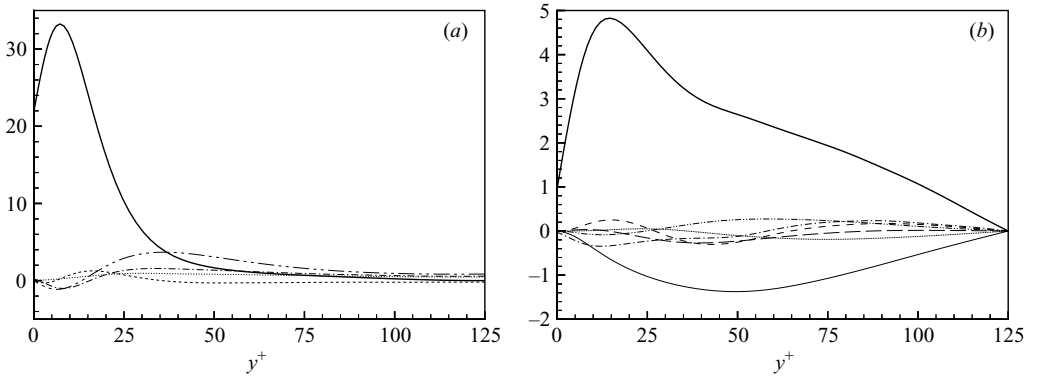

FIGURE 2. (*a*) Comparison of the term $S\langle R_{xy}\rangle$ (thick solid line) to the terms present in Φ_{xx} in equation (3.5), namely $\langle\partial_y(u_y R_{xx})\rangle$ (dashed line), $2\langle R_{xx}\partial_x u_x\rangle$ (dotted line), $2\langle R_{xy}\partial_y u_x\rangle$ (dash-dotted line), $2\langle R_{xz}\partial_z u_x\rangle$(dash-double-dotted line). Note that up to $y^+\sim 30\, S\langle R_{xy}\rangle$ is much larger than any other contribution. As (*a*) but (*b*) for $S\langle R_{yy}\rangle$ (thick solid line) compared with $\langle\partial_y(u_y R_{xy})\rangle$ (dashed line), $\langle R_{xx}\partial_x u_y\rangle$ (dotted line), $\langle R_{yy}\partial_y u_x\rangle$ (dash-dotted line), $\langle -R_{xy}\partial_z u_z\rangle$ (dash-double-dotted line), $\langle R_{xz}\partial_z u_y\rangle$ (long-dashed line) and $\langle R_{yx}\partial_z u_x\rangle$ (solid line). The numerical simulation is performed for $\tau = 25.0$ and friction Reynolds number $Re_\tau = 125$.

In this paper, our basic idea is to recognize that in limit of large Deborah number τS the terms Φ_{xx} and Φ_{xy} on the right-hand sides of (3.5) and (3.6) can be neglected. This statement can be checked against DNS of the FENE-P model. A description of the DNS is given in De Angelis *et al.* (2003). In figure 2(*a*) we compare the term SR_{xy} to the different contributions to Φ_{xx}, while in figure 2(*b*) we compare SR_{yy} to the terms which contribute to Φ_{xy}. In both cases, the term proportional to S is much larger than any other contribution in the viscoelastic layer, which allows us to neglect the terms Φ_{xx} and Φ_{xy} in (3.5) and (3.6) respectively, i.e. we obtain

$$\langle P R_{xx}\rangle = \tau S\langle R_{xy}\rangle, \tag{3.7}$$

$$\langle P R_{xy}\rangle = \tau S\langle R_{yy}\rangle. \tag{3.8}$$

Using equations (3.7), (3.8), we can rewrite our momentum balance equation in the form

$$\nu(y)S + W = p'L, \tag{3.9}$$

with the 'effective viscosity' being identified as

$$\nu(y) \equiv \nu_s + c_1\nu_p\langle R_{yy}\rangle. \tag{3.10}$$

It is a crucial and important observation that, while the stretching of polymers is given by the trace of R_{ij}, the effective viscosity appearing in the momentum balance depends only on $\langle R_{yy}\rangle$.

3.2. *The energy balance equation*

Next we derive the balance equation for energy. For this purpose, we will employ a phenomenological equation describing the balance between turbulent energy production WS and turbulent energy dissipation. The energy dissipation is estimated differently in the viscous boundary layer near the wall and in the bulk of the turbulent flow. In the absence of polymers, the balance equation is

$$a\nu\frac{K}{y2} + b\frac{K^{3/2}}{y} = WS \tag{3.11}$$

where $K \equiv \frac{1}{2}\sum_i u_i^2$. In equation (3.11) the second term on the left-hand side represent the standard Kolmogorov-type estimate of the energy flux and dissipation as the typical energy at distance y from the wall over the typical eddie turnover time $y/\sqrt{K}$. When there are no polymers acting in the system, equation (3.11) can be used with the momentum equation to obtain a closed set of equations describing the momentum flux and the mean shear, which in Prandtl units is

$$S^+ + W^+ = 1, \tag{3.12}$$

$$\frac{\delta^{+2}}{y^{+2}} + \frac{W^{+3/2}}{\kappa_N y^+} = W^+ S^+, \tag{3.13}$$

where $\kappa_N \equiv b/c_N^3$ is the von-Kármán constant, $\delta^+ \equiv \sqrt{a}/c_N$, while $c_N \equiv K/W$ is assumed to be a constant fixed by experimental data. For y^+ much larger than the viscous boundary layer near the wall (i.e. δ^+), equations (3.12), (3.13) provide the well-known von-Kármán solution for wall-bounded turbulent flow. For a suitable choice of c_N^2, equations (3.12), (3.13) can be considered rather good in reproducing the whole profile of the mean flow $V^+(y^+)$, from $y^+ = 0$ to the von-Kármán profile. This is shown in figure 1(*a*) as a solid black line. In the following, we consider equation (3.11) as a good candidate to represent the basic feature of the balance between turbulent production and turbulent energy dissipation.

In order to generalize equation (3.11) for the FENE-P model, we note that the overall dissipation of energy due to polymer stretching can be rigorously derived from equations (2.1) and (2.3). The final result is

$$E_p = \frac{\nu_p}{2\tau^2}\langle P^2 R_{\gamma\gamma}\rangle, \tag{3.14}$$

where $R_{\gamma\gamma} \equiv R_{xx} + R_{yy} + R_{zz}$.

As stated in (3.1), we represent the velocity field as the sum of its mean and the fluctuation, and consider separately the balance equation for the mean energy V^2 and for the turbulent energy $\langle u^2\rangle$. The former yields an equation identical to (3.2) but multiplied by S:

$$WS + \nu_s S^2 + \frac{\nu_p}{\tau}\langle P R_{xy}\rangle(y) S = p' L S. \tag{3.15}$$

Thus the contribution of the polymer to the dissipation of the velocity fluctuations, denoted as ϵ_p, is finally of the form

$$\epsilon_p = \frac{\nu_p}{2\tau^2}\langle P^2(R_{xx} + R_{yy} + R_{zz}) - 2\langle P R_{xy}\rangle S\tau\rangle. \tag{3.16}$$

It is important to realize that this equation embodies an important cancellation. To see this we return to (2.1), multiply it by P, use (3.7) and derive

$$\frac{1}{\tau}\langle P^2 R_{xx}\rangle = 2\langle P R_{xy}\rangle S. \tag{3.17}$$

Thus, there is an exact cancellation in (3.16) between the first and the fourth terms. We can thus safely proceed to write the balance equation for the turbulent energy in the presence of polymer stretching:

$$a\nu\frac{K}{y^2} + b\frac{K^{3/2}}{y} + \frac{\nu_p}{2\tau^2}\langle P^2(R_{yy} + R_{zz})\rangle = WS. \tag{3.18}$$

Finally, we refer again to our DNS results to assess the relative importance of $\langle R_{yy}\rangle$ and $\langle R_{zz}\rangle$: these are very close to each other throughout the region of concern in the

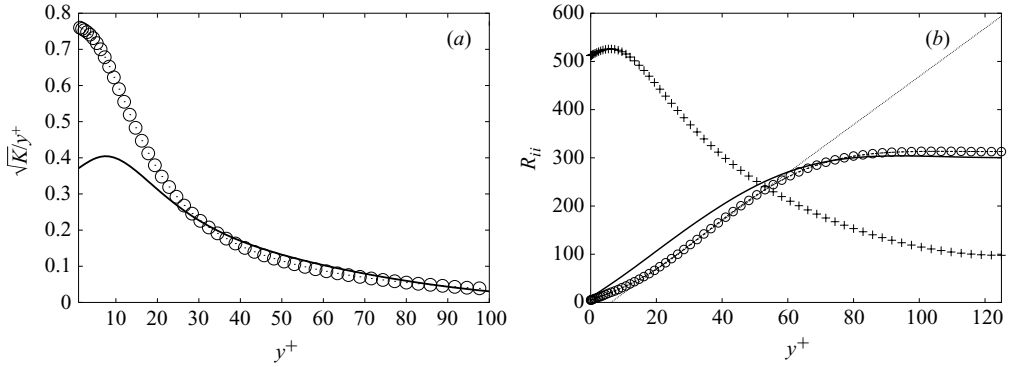

FIGURE 3. (*a*) $\sqrt{K}/y^+$ (circles) as a function of y^+ as obtained in the DNS of the FENE-P model. The continuous line shows $C_2\langle P\rangle/\tau$ ($C_2 \sim 6.5$) computed for the same numerical simulation. Note that outside the viscous boundary layer $y^+ \leqslant 10$, the estimate $\sqrt{K}/y^+ \sim \langle P\rangle/\tau$ is quite well satisfied. (*b*) $\langle R_{xx}\rangle$ (crosses), $\langle R_{yy}\rangle$ (circles) and $\langle R_{zz}\rangle$ (black continuous line) as obtained by direct numerical of the FENE-P model. We have multiplied $\langle R_{yy}\rangle$ and $\langle R_{zz}\rangle$ by 10 and by 6, respectively, to improve readability. Note that $\langle R_{zz}\rangle \sim \langle R_{yy}\rangle$ for almost all values of y^+ and that $\langle R_{yy}\rangle \sim y$ (represented by the thin line) up to $y^+ \sim 50$.

channel, as shown in figure 3. We therefore can keep only one of them at the expense of the introduction yet another constant of the order of unity:

$$a\nu\frac{K}{y^2} + b\frac{K^{3/2}}{y} + \frac{c_3\nu_p}{\tau^2}\langle P^2 R_{yy}\rangle = WS. \tag{3.19}$$

To bring the equation into a more convenient form, we recall that the coil–stretch transition is expected to occur when the effective relaxation time τ/P of the polymer is of the order of the typical time scale for the velocity fluctuations, $y/\sqrt{K(y)}$; the coil–stretch transition is a necessary condition for a strong interaction of the polymers with the flow, and thus of drag reduction. In figure 3(*a*) we plot $\sqrt{K}/y$ and $\langle P\rangle/\tau$ to show the quality of our estimate. This indicates that the third term on the left-hand side of (3.19) can be estimated as

$$\frac{c_3\nu_p}{\tau^2}\langle P^2 R_{yy}\rangle \cong \frac{c_3\nu_p}{\tau^2}\langle P\rangle^2\langle R_{yy}\rangle = c_4\nu_p\langle R_{yy}\rangle\frac{K(y)}{y^2}. \tag{3.20}$$

Thus, the energy balance equation can be also written in terms of an effective viscosity, in a similar way to the momentum balance equation, namely

$$a\tilde{\nu}(y)\frac{K}{y^2} + b\frac{K^{3/2}}{y} = WS, \tag{3.21}$$

$$\tilde{\nu}(y) \equiv \nu_s + c_4\nu_p\langle R_{yy}\rangle. \tag{3.22}$$

Comparing with (3.10) we see that $\nu_p\langle R_{yy}\rangle$ serves as the effective viscosity in this problem.

Let us summarize our finding and the basic assumptions made so far. First, we have used equations (3.7) and (3.8), neglecting Φ_{xx} and Φ_{xy} which are considered small for $De \to \infty$. We supported this approximation by showing in figure 2 the relative importance of the various terms as obtained in a DNS of the FENE-P model. Next, we assume that the term $\sqrt{K}/y$ appearing in the energy balance equation can be estimated as P/τ, i.e. as the effective relaxation time of the polymers. This assumption is based on the idea that, at large enough Deborah number, the polymers undergo a

coil–stretch transition. Finally, we employ a rather straightforward approximation by computing $R_{yy}+R_{zz}$ as $c_3 R_{yy}$, with c_3 a suitable constant of order 1. This approximation is based on the fact that R_{yy} and R_{zz} have a similar behaviour as function of y, supported by DNS of the FENE-P equations and shown in figure 3. Based on the above discussion, we reach the important conclusion that the overall effect of polymers in turbulent boundary layers is physically equivalent to introducing an effective viscosity proportional to R_{yy}.

3.3. *The MDR asymptote*

At this point we have the same balance equations that were employed by L'vov *et al.* (2004), and the derivation of the MDR, following the same reasoning, is briefly reviewed in the following. As in the Newtonian theory one needs to add a phenomenological relation between $W(y)$ and $K(y)$,

$$W(y) = c_V^2 K(y), \tag{3.23}$$

whereas in the Newtonian theory we have the rigorous bound $c_V \leqslant 1$ (L'vov *et al.* 2004).

Using (3.23) we can estimate $W = c_V^2 K \sim y^2 \langle P \rangle^2 / \tau^2$ and, consequently for small y and large value of $\langle P \rangle / \tau$ (i.e. at the MDR) the first term on the left-hand side of (3.9) is dominant and we find (assuming that the kinematic viscosity is negligible) $c_1 v_p \langle R_{yy} \rangle \approx p' L / S(y)$. Substituting this in the first term on the left-hand side of (3.21), we obtain the estimate

$$S(y) \approx c_5 p' L / y, \tag{3.24}$$

which leads to a logarithmic solution for $V(y)$. The derivation of the MDR in reduced variables gives the final result

$$V^+(y^+) = \frac{1}{\kappa_V} \ln(e \kappa_V y^+), \tag{3.25}$$

where e is the Neper number and $\kappa_V \equiv c_V/(c_N y_v^+)$. In this expression y_v^+ is the cross-over point between the viscous region and the von-Kármán log law of the wall in the Newtonian problem. As a consequence of our derivation, we obtain that $R_{yy} \sim 1/S \sim y$, i.e. the effective viscosity should grow linearly with respect to distance from the wall. In figure 3 we show that $\langle R_{yy} \rangle \sim y$, as predicted. Let us remark that the work done so far enables us to the FENE-P equations in a physical way and to understand how the different components of the conformation tensor R_{ij} play different roles in the mechanism of drag reduction. The next step is to understand the effect of varying the concentration of polymers.

4. Saturation of drag reduction and cross-over from the MDR to the Newtonian plug

Experimentally mean velocity profile is seen to follow the MDR up to some point y_V^+ after which it crosses back to a logarithmic profile with the same slope as the Newtonian flow. To measure the amount of drag reduction one can introduce a dimensionless drag reduction parameter

$$Q \equiv \frac{y_V^+}{y_N^+} - 1. \tag{4.1}$$

The Newtonian flow is then a limiting case of the viscoelastic flow corresponding to $Q = 0$.

We expect a cross over from the MDR asymptote back to the Newtonian plug when the basic assumptions on the relative importance of the various terms in the balance equations lose their validity, i.e. when (i) the turbulent momentum flux W becomes comparable with the total momentum flux $p'L$, or (ii) the turbulent energy flux $bK^{3/2}/y$ becomes of the same order as the turbulent energy production WS. Using the estimates (3.24) and $K = c_V^2 W \sim y^2 \langle P \rangle^2 / \tau^2$, one can show that both these conditions give the same cross-over point y_V, namely

$$y_V \simeq \frac{\tau \sqrt{p'L}}{\langle P \rangle}. \tag{4.2}$$

Let us denote $\tilde{\tau}(y) \equiv \tau / \langle P(y) \rangle$ the effective nonlinear polymer relaxation time. Then condition (4.2) can be also rewritten as

$$S(y_V)\tilde{\tau}(y_V) \simeq 1. \tag{4.3}$$

In writing this equation we use the fact that the cross-over point also belongs to the edge of the Newtonian plug where $S(y) \approx \sqrt{p'L}/y$. The left-hand side of this equation is simply the local Deborah number (the product of local mean shear and local effective polymer relaxation time). Thus, *the cross-over to the Newtonian plug ocuurs at the point, where the local Deborah number decreases to* ~ 1. We expect that this result is correct for any model of elastic polymers, not only for the FENE-P model considered here.

To understand how the cross-over point y_V depends on the polymer concentration and other parameters, we need to estimate the mean value of the Peterlin function $\langle P \rangle$. Note that a change in the concentration $c_p = \nu_p/\nu_0 \to \lambda \nu_p/\nu_0$ is equivalent, in the FENE-P equations, to $R_{ij} \to \lambda R_{ij}$ and $\alpha \to \alpha/\lambda$. Therefore, the limit $c_p \to \infty$ is equivalent to $\alpha \to 0$, i.e. to $P \to 1$, while the limit $c_p \to 0$ implies $\alpha \to \infty$ and therefore even a small amount of stretching will produce a large value of P. Thus the basic properties of the FENE-P model predict that $P \to \infty$ for small concentration and $P \to 1$ for large enough concentration (see also Benzi *et al.* 2004*a*). Using (4.2) we immediately see that for small concentration $y_V \to 0$ while for large concentration y_V reach its maximum value given by $\tau\sqrt{p'L}$. In the following, we discuss how the same exact results are obtained by using the theory discussed in the previous section.

Using (2.3) and the estimate $\langle R \rangle = \langle R_{xx} + R_{yy} + R_{zz} \rangle \sim \langle R_{xx} + 2R_{yy} \rangle$, it follows from (3.8) and (3.7) that

$$\langle R_{xx} \rangle \simeq (S\tilde{\tau})^2 \langle R_{yy} \rangle,$$

and at the cross-over point (4.3)

$$\langle R_{xx} \rangle \simeq \langle R_{yy} \rangle, \quad \langle R \rangle \simeq 3\langle R_{yy} \rangle.$$

The dependence of $\langle R_{yy} \rangle$ on y in the MDR region follows from (3.19) and (3.24):

$$\langle R_{yy} \rangle \simeq \frac{\tilde{\tau}^2 WS}{\nu_p} \simeq \frac{y\sqrt{p'L}}{\nu_p}.$$

Then at the cross-over point $y = y_V$

$$\langle P \rangle \simeq \frac{1}{1 - 3\alpha y_V \sqrt{p'L}/\nu_p}.$$

Substituing this estimation into (4.2) gives the final result

$$y_V = \frac{C\tau\sqrt{p'L}}{1+\alpha p'L\tau/\nu_p}. \tag{4.4}$$

Here C is a constant of the order of unity. Finally, introducing the dimensionless concentration of polymer

$$\tilde{c}_p \equiv \frac{\nu_p}{\alpha\,\nu_0}, \tag{4.5}$$

one can write the denominator in (4.4) as

$$1+\frac{\alpha p'L\tau}{\nu_p} = 1+\frac{1}{\tilde{c}_p}\frac{p'L\tau}{\nu_0} = 1+\frac{De}{\tilde{c}_p},$$

where

$$De \equiv \frac{p'L\tau}{\nu_0} \tag{4.6}$$

is the (global) Deborah number. Then for the dimensionless cross-over point $y_V^+ \equiv y_V\sqrt{p'L}/\nu_0$ one obtains

$$y_V^+ = \frac{CDe}{1+De/\tilde{c}_p}. \tag{4.7}$$

There are two non-trivial predictions which can be tested by using equation (4.7). For small values of $\tilde{c}_p$, y_V^+ is linear in $\tilde{c}_p$, i.e. drag reduction has a linear relation with the polymer concentration. On the other hand, for large value of $\tilde{c}_p$, the FENE-P model becomes equivalent to the Oldroyd B model ($P = 1$) (Benzi *et al.* 2004*a*) and one should observe an increase of drag reduction proportional to De. Indeed, in numerical simulations when the Deborah number De was changed systematically, cf. Yu *et al.* (2001), the cross-over was observed to depend on De in a manner consistent with (4.7). The other limit when $\tilde{c}_p$ is very small was discussed in full detail in Benzi *et al.* (2004). The main result of Benzi *et al.* (2004*b*) is that the drag reduction parameter Q is given by

$$Q = l_p^3 c_p N_p^3 \quad c_p \text{ small}, \quad Re \text{ large}, \tag{4.8}$$

where N_p is the degree of polymerization (the number of monomers per molecule) and l_p is the linear scale of the monomer. This prediction was tested in Benzi *et al.* (2004*b*) by comparing with experiments with DNA as the drag reducing agent, with excellent agreement between theory and experiments.

We can thus reach conclusions about the saturation of drag reduction in various limits of the experimental conditions, in agreement with experiments and simulations.

5. Conclusions

In this paper we present a theoretical framework aimed at understanding drag reduction for wall-bounded turbulent flow in dilute polymer solution. We based our results on a few approximations and the idea that the polymers undergo a coil–stretch transition for large enough polymer length and Reynolds number. DNS of the FENE-P model confirm the very good quality of the approximations made.

There are two major results obtained in the paper. First, we highlight the different physical role played by the different components of the conformational tensor R_{ij}, and in particular we show that $\langle R_{yy}\rangle$ appears in the balance equations as an effective viscosity. It is important to realize that it is this component and not R_{xx}, which is in

fact much larger (by a factor of De^2), that enters the theory. Indeed, one simple and non-trivial prediction of our theory is that $\langle R_{yy} \rangle \sim y$ close to the wall. It is known that the overall stretching of the polymers (i.e. the trace of R_{ij}) decreases as a function of y, but this is mainly due to the decay of $\langle R_{xx} \rangle$. Nevertheless, R_{yy} is predicted to increase linearly with y, in very good agreement with DNS. Second, we are able to predict how drag reduction depends on polymer concentration and how eventually, for large enough concentration, the drag reduction reaches its limiting value given by the so called MDR asymptote.

In our discussions, we employed very simple balance equations for the momentum and energy production and energy dissipation in wall-bounded turbulent flow. We propose therefore that most of our results, if not all, are model independent.

This work was supported in part by the European Commission under a TMR grant, the US-Israel Binational Science Foundation, and the Minerva Foundation, Munich, Germany.

REFERENCES

Benzi, R., Ching, E., Horesh, N. & Procaccia, I. 2004*a* Theory of concentration dependence in drag reduction by polymers and of the MDR asymptote. *Phys. Rev. Lett.* **92**, 078302.

Benzi, R., L'vov, V. S., Procaccia, I. & Tiberkevich, V. 2004*b* Saturation of turbulent drag reduction in dilute polymer solutions. *Europhys. Lett.* **68**, 825.

Beris, A. N. & Edwards, B. J. 1994 *Thermodynamics of Flowing Systems with Internal Microstructure.* Oxford University Press.

Bird, R. B., Curtiss, C. F., Armstrong, R. C. & Hassager, O. 1987 *Dynamics of Polymeric Fluids*, Vol. 2. Wiley.

De Angelis, E., Casciola, C. M., L'vov, V. S., Piva, R. & Procaccia, I. 2003 Drag reduction by polymers in turbulent channel flows: energy redistribution between invariant empirical modes. *Phys. Rev.* E **67**, 056312.

De Angelis, E., Casciola, C., L'vov, V. S., Pomyalov, A., Procaccia, I. & Tiberkevich, V. 2004 Drag reduction by a linear viscosity profile. *Phys. Rev.* E **70**, 055301.

L'vov, V. S., Pomyalov, A., Procaccia, I. & Tiberkevich, V. 2004 Drag reduction by polymers in wall bounded turbulence. *Phys. Rev. Lett.* **70**, 026304.

L'vov, V. S., Pomyalov, A., Procaccia, I. &. Tiberkevich, V. 2005 The polymer stress tensor in turbulent shear flow. *Phys. Rev.* E **71**, 061305.

Lumley, J. L. 1969 Drag reduction by additive. *Annu. Rev. Fluid Mech.* **1**, 367.

Pope, S. C. 2000 *Turbulent Flows.* Cambridge University Press.

Rollin, A. & Seyer, F. A. 1972 Velocity measurements in turbulent flow of viscoelastic solutions. *Can. J. Chem. Engng* **50**, 714.

Rudd, M. J. 1969 Measurements made on a drag reducing solution with a laser velocimeter. *Nature* **224**, 587.

Sreenivasan, K. R. & White, C. M. 2000 The onset of drag reduction by dilute polymer additive, and the maximum drag reduction asymptote. *J. Fluid Mech.* **409**, 149.

Virk, P. S. 1969 Drag reduction fundamentals. *AIChE J.* **21**, 625.

Yu, B., Kawaguchi, Y., Takagi, S. & Matsumoto, Y. 2001 DNS study on the drag reducing flow with additives employing Giesekus fluid model and MINMOD scheme: effect of Weissenberg number on the turbulent flow structure. *7th Symposium on Smart Control of Turbulence, University of Tokyo.*

Warholic, M. D., Massah, H. & Hanratty, T. J. 1999 Influence of drag reduction by polymers on turbulence: effects of Reynolds number, concentration and mixing. *Exps. Fluids* **27**, 461.